





## Fire may prevent future Amazon forest recovery after large-scale deforestation

Markus Drüke <sup>1</sup>✉, Boris Sakschewski <sup>1</sup>, Werner von Bloh<sup>1</sup>, Maik Billing<sup>1</sup>, Wolfgang Lucht <sup>1</sup> & Kirsten Thonicke <sup>1</sup>

The Amazon forest is regarded as a tipping element of the Earth system, susceptible to a regime change from tropical forest to savanna and grassland due to anthropogenic land use and climate change. Previous research highlighted the role of fire in amplifying irreversible large-scale Amazon die-back. However, large-scale feedback analyses which integrate the interplay of fire with climate and land-use change are currently lacking. To address this gap, here we applied the fire-enabled Potsdam Earth Model to examine these feedback mechanisms in the Amazon. By studying forest recovery after complete deforestation, we discovered that fire prevents regrowth across 56-82% of the potential natural forest area, contingent on atmospheric carbon dioxide levels. This emphasizes the significant contribution of fire to the irreversible transition, effectively locking the Amazon into a stable grassland state. Introducing fire dynamics into future assessments is vital for understanding climate and land-use impacts in the region.

<sup>1</sup>Potsdam Institute for Climate Impact Research, Member of the Leibniz Association, Telegraphenberg A31, 14473 Potsdam, Germany.  
✉email: [drueke@pik-potsdam.de](mailto:drueke@pik-potsdam.de)

The Amazon basin contains about 40% of the world's tropical forest area. It plays an important role in providing vital ecosystem services and stabilizing Earth's climate system<sup>1</sup> by storing about 10% of the global forest carbon, sequestering about 5% of historic human CO<sub>2</sub> emissions, and recycling ca. 20–40% of its rainfall<sup>2</sup>.

In the past decades, human activity imposed growing pressure on the functionality of the Amazon forest. Anthropogenic land-use change has reduced forest cover by ca. 20% of the Amazon basin, with negative impacts on associated ecosystem services<sup>3</sup>. Additionally, increasing droughts and temperature stress, along with logging and slash-and-burn practices, threaten the survival of large areas of the Amazon<sup>4–10</sup>. A potential die-back of the Amazon forest was first described by ref. <sup>11</sup> and later investigated by e.g., refs. <sup>6,12,13</sup>. Lovejoy et al.<sup>14</sup> argued in 2018 that developments in the region are close to crossing a tipping point if land use expansion is not immediately halted. Such tipping could be accelerated by self-reinforcing feedback mechanisms, such as the coupling of climate change and increasing fire regimes, which could push the Amazon tropical forest to a savanna-like or treeless state. These resulting grassland or dry forest regions would burn more frequently and intensely, thus leading to a lock-in effect and preventing recovery from the treeless state<sup>9,15</sup>. Similarly, the collapse of Amazon moisture recycling due to deforestation could decrease precipitation over the Amazon basin and potentially prevent the regrowth of trees<sup>16,17</sup>. Other mechanisms, such as increased plant growth due to CO<sub>2</sub> fertilization, could partially offset the negative impacts of climate change on the forest, but the magnitude of this effect remains uncertain to date<sup>18</sup>.

While the die-back of the Amazon forest and the role of fire in stabilizing grassland ecosystems have long been known and studied, the interactions and feedback mechanisms between fire, vegetation, and climate simultaneously have mainly been missing, with studies largely based on remote sensing data<sup>19</sup>, conceptual models<sup>20</sup> or models of reduced complexity<sup>9,16,17,21</sup>. Furthermore, the long-term effects of fire on Amazon forest recovery are often neglected, and, if at all, studies focused on past decades or short future time scales of at most 100 years<sup>22,23</sup>. However, as tropical forest recovery might take centuries to regain forest biomass, moisture recycling networks, and other ecosystem functions, current findings are based on too short time scales<sup>24</sup>.

Here, we study the role of fire in a multi-century trajectory of Amazon forest recovery after complete deforestation and different levels of atmospheric CO<sub>2</sub> concentrations by employing the fire-enabled Earth system model POEM (in the configuration CM2Mc-LPJmL v1.0<sup>25</sup>). Using the coupled system allows us to analyze the effects of climate change, fire, and land-use change simultaneously. In this model, the dynamic vegetation is simulated by the coupled state-of-the-art dynamic global vegetation model LPJmL<sup>26</sup>, with its embedded process-based fire model SPITFIRE<sup>27,28</sup>. Simulated fire occurrence highly depends on the vegetation type, its moisture, and tree architecture, which is modeled by LPJmL (along with prescribed population density and lightning activity for computing ignitions), while fire-induced mortality affects vegetation dynamics within LPJmL. Both, vegetation dynamics and fire occurrence, are further impacted by climate and influence the atmosphere through changes in the water and energy cycle.

Our experimental setup covers three simulation phases (see Fig. 1 and Methods): The first phase (hereafter: spin-up phase) reflects a standard procedure letting global vegetation and climate equilibrate together. In the second phase (hereafter: grassland phase), the area of the Amazon basin is completely deforested and only grass is allowed to grow. In the third phase, trees are allowed to recover (hereafter: recovery phase). The model experiments are

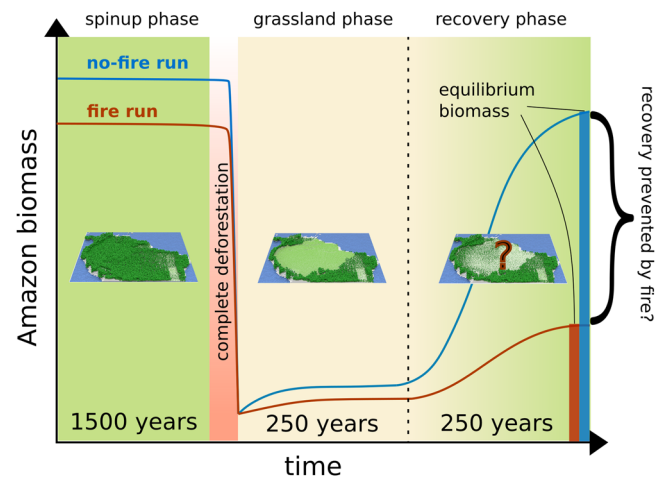


**Fig. 1 Conceptual experimental design for testing the influence of fire on the Amazon regrowth potential.** After bringing climate and vegetation into equilibrium over 1500 years under historical atmospheric CO<sub>2</sub>

concentrations (spin-up phase), for two model set-ups (with and without fire), all trees in the Amazon region are removed and only grass can grow for 250 simulation years (grassland phase). It is followed by another 250 simulation years where trees are allowed to grow again (recovery phase). At the end of the last simulation phase, the relative difference in biomass between the model set-ups is taken, which denotes the role of fire in preventing forest recovery (illustrated by red vs. blue bar). The whole simulation is performed multiple times from the grassland phase onwards under different constant atmospheric CO<sub>2</sub> concentrations to assess the influence of climate and CO<sub>2</sub> fertilization on forest recovery.

performed for a number of different constant atmospheric CO<sub>2</sub> concentrations (284, 450, 750, and 1200 ppm) and with fire either enabled or disabled. Furthermore, for all experiments, additional control experiments were performed, which have the same fire ignition and climate forcing but are simulated without deforestation. Fire ignitions in the Amazon are adapted to match typical ignition dynamics in deforested areas in South America (see Methods).

In these idealized experiments, we intended to investigate whether the fire is an important factor in the recovery from an Amazon grassland state, including potential irreversibility. We here deliberately choose the two most extreme scenarios, to investigate the span of potential responses in the Earth system. In the real world, those responses will most likely have a more complex and heterogenous spatial pattern with impacts situated somewhere in between the bounds of our extreme scenarios. As current Earth system models (including POEM), are not yet able to quantify exact atmospheric CO<sub>2</sub> concentrations, at which e.g. an Amazon tipping would occur or the exact areal extent, where vegetation regrowth would be prevented, it is the aim of this study to contribute to a better system understanding and analysis of the role of fire in climate vegetation interactions in South America and overall responses and processes of the Earth system.

We find that a warmer and drier regional climate caused by the grassland state increases fire activity, which locks large parts of the Amazon forest into the grassland state and prevents forest recovery. In the experiments without fire, the forest was able to recover within 250 years, which emphasizes the important role of fire in the irreversibility of tropical deforestation. Our results highlight the need to keep the Earth's system within stable boundaries and limit climate change as well as tropical deforestation in order to prevent the tropical forest from crossing an irreversible fire-controlled tipping point.

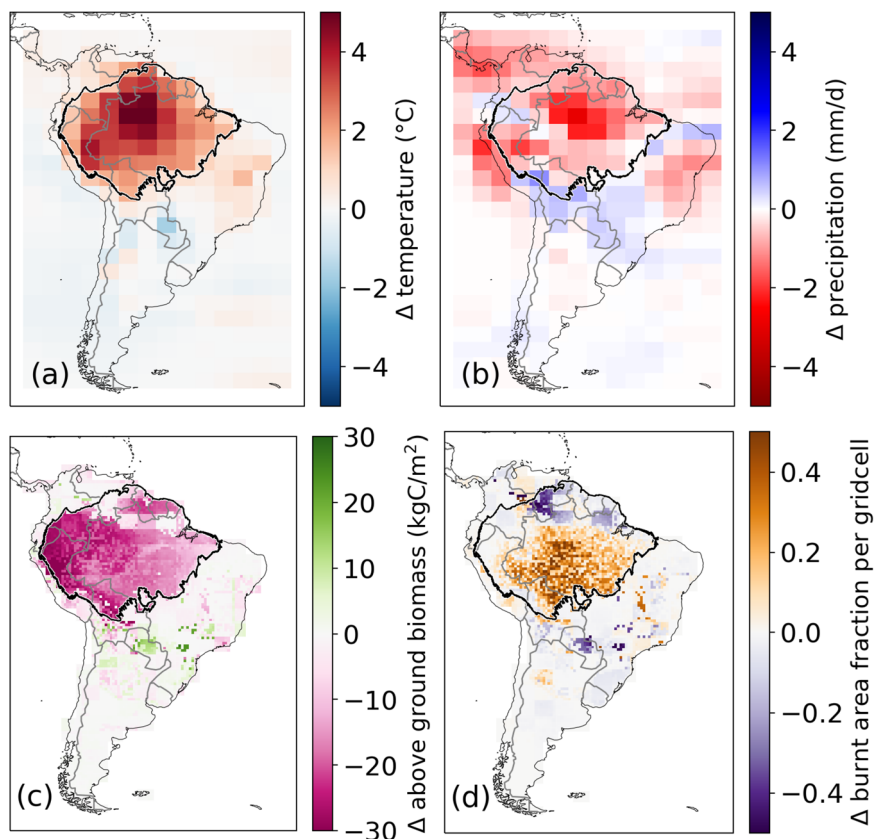


**Fig. 2 Effect of the grassland phase on climate, vegetation, and fire.** Difference between the grassland phase and the control experiment, both at 450 ppm atmospheric CO<sub>2</sub> concentration and with activated fire disturbance, for the simulated annual mean **a** surface temperature, **b** precipitation, **c** aboveground biomass, and **d** fractional burnt area averaged over the last 10 simulation years of the grassland phase. The extent of the deforested Amazon basin is marked with black outlines. In the grassland state, decreased precipitation and increased temperature led to an increase in burnt areas.

## Results and discussion

**Effects of deforestation on climate and fire in the Amazon forests (grassland phase).** The deforestation of the entire Amazon region and allowing only grass to grow thereafter (grassland phase) showed large differences to the respective control experiments due to biophysical feedback between climate, vegetation, and fire (Fig. 2 and Figs. S3–S5). Under 450 ppm atmospheric CO<sub>2</sub> concentration, for example, the aboveground biomass in the Amazon decreased strongly, as grasslands only store ca. 1–3 kgC m<sup>-2</sup> in aboveground biomass, compared to 20–30 kgC m<sup>-2</sup> in the Amazon tropical forest (Fig. 2c). Moreover, air temperature in the central Amazon increased by ca. 4 °C (Fig. 2a) while overall precipitation was lower by 1–2 mm day<sup>-1</sup> over the basin compared to the control experiment (for other CO<sub>2</sub> levels, see corresponding panels in S3–S5). These changes are within the range of previous studies, which found warming of 4.2 °C and a precipitation reduction of ca 1 mm day<sup>-1</sup> for the eastern Amazon in case of complete deforestation<sup>29</sup>, or warming by more than 3 °C alongside a strong precipitation reduction, especially during the dry season from July to November<sup>8</sup>.

Driven by the biophysical coupling, reduced evapotranspiration resulting from grasslands replacing forests, generally lowers latent heat loss and causes local warming<sup>30</sup>. On the other hand, the albedo of grass is usually higher than the albedo of a closed forest (such as the Amazon), which results in a slight cooling<sup>31</sup>. We found the first effect to be dominant in our simulations, which resulted in net warming. The reduced evapotranspiration also caused a decrease in humidity, lowering annual precipitation over the Amazon region. Evapotranspiration is lower in

grasslands compared to forests because of their shallower roots and reduced leaf rainfall interception<sup>32</sup>.

The warmer and drier climatic conditions increased the average annual burned area by a factor of 2–3 in the Amazon basin (Fig. 2d), especially in the southern Amazon. In contrast, some extremely hot and dry parts in the northern Amazon showed reduced burned area due to inhibited grassland productivity and, thus, fuel limitation. In the western Amazon, wetter conditions persisted and the fire regime did not change substantially. The difference in burnt area is spatially heterogeneous as a result of the relatively random characteristics of human ignition forcing in the model (see Methods).

## Fire prevents a complete recovery of the Amazon forest (recovery phase).

After the 250 years-long grassland phase, trees were allowed to re-establish in the Amazon region in the final simulation phase of 250 years (recovery phase). Without fire, ca. 95% of the original biomass recovered in all scenarios tested except under the 1200 ppm scenario, which regained only ca. 80% of the corresponding control experiment (Figs. 3, 4a–d and Supplementary Video 1). For the latter, extremely dry and hot conditions persisted in parts of the northern Amazon such that extreme heat stress on woody vegetation prevented forest recovery (for simulated biomass of the control experiments, see Figs. S1, S2 and for all time series and absolute values, see Figs. S7, S8).

The addition of fire to the simulation experiments reduced the average biomass recovery in the Amazon basin strongly. Biomass recovered to only ca. 40% at 284 ppm (50% at 450 ppm, 50% at

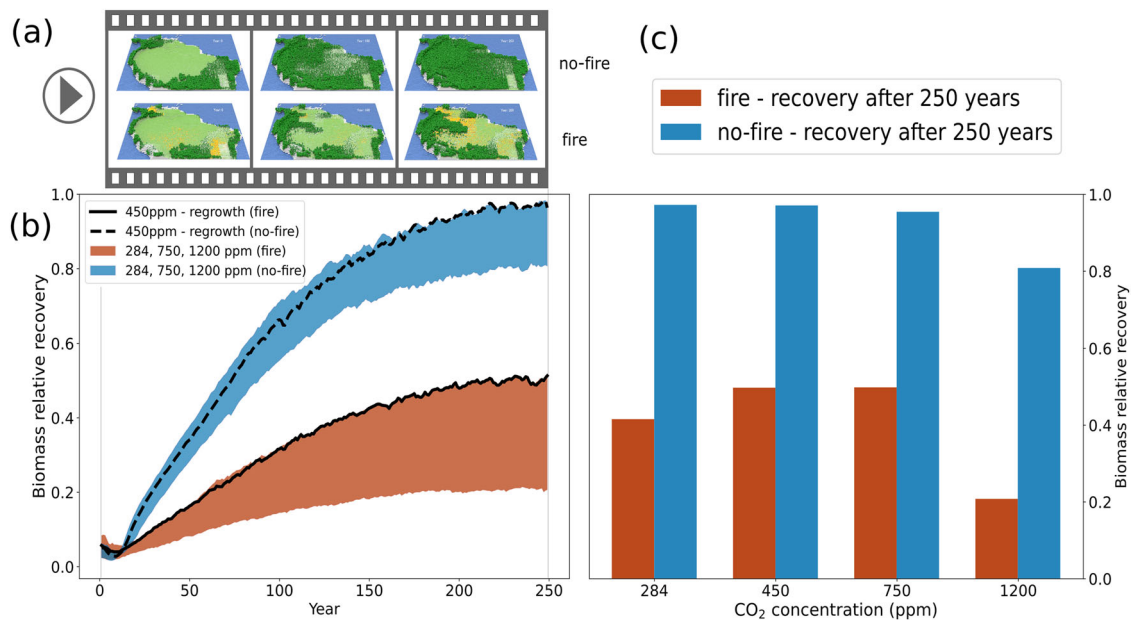


**Fig. 3** The effects of fire and climate change on biomass regrowth in the recovery phase. **a** Biomass/fire maps at the beginning (left panels), after 120 years (central panels), and at the end of the recovery phase (right panels, snapshots taken from Supplementary Video 1: [www.pik-potsdam.de/~drucke/fire\\_nofire\\_combined.mkv](http://www.pik-potsdam.de/~drucke/fire_nofire_combined.mkv)). **b** Time series of biomass recovery. Without fire (dashed line for 450 ppm and blue area for other CO<sub>2</sub> concentrations), biomass nearly fully recovers under 284, 450, and 750 ppm, respectively, but only 80% under 1200 ppm. Fire (solid line for 450 ppm and red area for other CO<sub>2</sub> concentrations) inhibits full biomass recovery, with only 20% (at 1200 ppm), 40% (at 284 ppm), and 50% (at 450 ppm and 750 ppm) of biomass recovered after 250 years. **c** Bar plot showing final relative biomass under different atmospheric CO<sub>2</sub> concentration forcing (mean of the last 10 years of the recovery phase). Biomass is normalized to its corresponding control simulation experiment (same atmospheric CO<sub>2</sub> concentration).

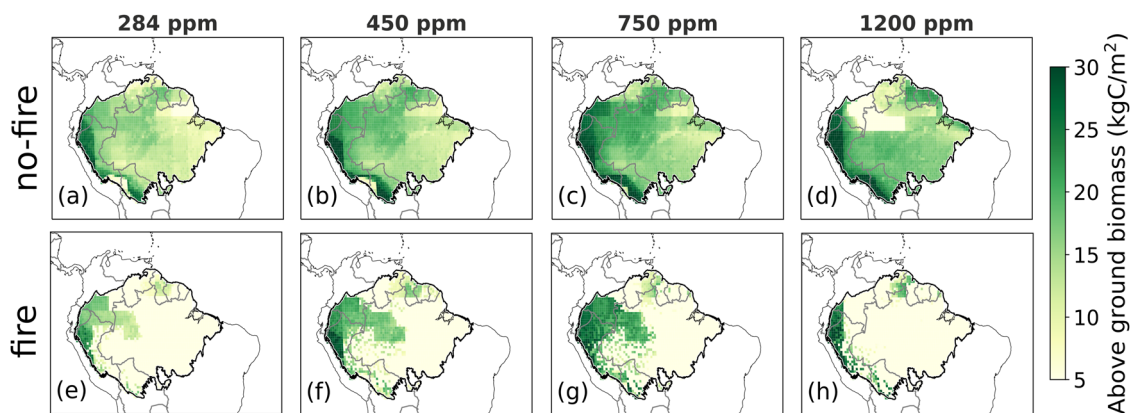


**Fig. 4** Regrowth of the Amazon in the recovery phase. Modeled mean aboveground biomass over the last 10 years of the recovery phase for no-fire (**a–d**) and with fire (**e–h**) under 284 ppm (**a, e**), 450 ppm (**b, f**), 750 ppm (**c, g**), and 1200 ppm (**d, h**). Biomass recovered homogeneously throughout the whole Amazon basin for the no-fire experiments, while the Amazon only recovered partially with fire disturbance enabled.

750 ppm, 20% at 1200 ppm, Fig. 3 and Table 1). More strikingly, 56–82% (353–515 Mio ha) of the Amazon area previously covered by forest could not recover to tropical forest and was locked in the grassland state at the end of the recovery phase (Table 1, Fig. 4e–h, PFT fractions see S6).

Through positive feedback mechanisms between fire, vegetation and climate, higher temperatures (Fig. 2a), and reduced precipitation (Fig. 2b) in the grassland state supported increasing fire activities (Fig. 2d), thereby maintaining a fire-prone and irreversible grassland state in large parts of the Amazon (e.g., in the eastern Amazon). In particular, the extreme climate in the 1200 ppm scenario led to such hot and dry conditions that almost all of the Amazon remained in the grassland state, except in the Andes region, where lower temperatures due to higher altitudes remained within the bioclimatic limits of tropical trees.

The difference in biomass recovery between the four CO<sub>2</sub> forcings was controlled by two opposing mechanisms: While a higher atmospheric CO<sub>2</sub> concentration increased the CO<sub>2</sub> fertilization effect and water use efficiency, and thus simulated forest growth<sup>18</sup>, it also increased global warming, and thus, the resulting heat stress decreased or prevented tree growth. The first mechanism was dominant for a CO<sub>2</sub> increase from 284 ppm to 450 and to 750 ppm, respectively, but the negative impact of heat stress prevented forest recovery to a large extent under the 1200 ppm experiment.

In simulations with enabled fire, the spatial pattern of forest recovery followed a heterogeneous pattern explainable by general moisture dynamics in the Amazon basin: First, forests started to establish and grow at the western border of the Amazon (see Supplementary Video 1). In the 284, 450, and 750 ppm scenarios,

**Table 1 Overview of the biomass recovered and the proportion of the area of the Amazon basin, which remained locked in the grassland state at the end of the recovery phase.**

Scenario	Biomass recovered	Area locked as grassland
<b>with fire</b>		
284 ppm	40%	400 Mio ha (69%)
450 ppm	50%	373 Mio ha (57%)
750 ppm	50%	353 Mio ha (56%)
1200 ppm	20%	515 Mio ha (82%)
<b>without fire</b>		
284 ppm	98%	10 Mio ha (1.5%)
450 ppm	97%	0 ha
750 ppm	95%	0 ha
1200 ppm	80%	71 Mio ha (10.5%)

The percent value is relative to the respective control experiment. A cell was assumed grassland with biomass below 5 kg C m<sup>2</sup>.

forest cover in the area in the western Amazon (close to the Andes) almost reached the state of the control experiment (Fig. 4e–h). Here, the moist air, channeling from the Atlantic Ocean towards the Andes, was releasing enough precipitation on the eastern side of the mountains, to foster relatively fast forest regrowth. Other regions, especially in the eastern Amazon, were more dependent on slowly re-establishing moisture recycling mechanisms supported by increasing forest cover, which is also proved by substantially lower annual precipitation in the grassland state (see Fig. 2)<sup>2,8,17,23</sup>. Re-establishing forest increased local evapotranspiration and consequently humidity, which incrementally restored climate conditions similar to the corresponding control experiment (with full forest cover, see Supplementary Video 1). Canopy closure further increased humidity, reduced wind speed, and thus lowered fire risk and consequently burnt area. Increasing forest cover also fostered the transport of moisture to the atmosphere, increased precipitation of neighboring cells downwind, and improved the conditions for tree growth. As a result, the average burned area declined in the first 50 years of the recovery phase in those areas, where forests re-emerged. Where large amounts of grasslands persisted, fire burned up to 50% of the grid cells. The average burnt area remained high throughout the recovery phase (ca. 18–20%) in the Amazon region compared to the control experiments (ca. 6–8%, Fig. 5 and S9). While fire leads to a much large fraction of the more fire-adapted rain green trees compared to more evergreen trees in the simulations without fire, larger fractions of grassland prevail at the end of the recovery phase, fostering a still relatively large fire regime (Figs. S7, S9).

Interestingly, fire activity was not higher in the 1200 ppm compared to the 750 ppm experiment, due to an extreme temperature increase at 1200 ppm (above 4 °C, Fig. S5). This increased the fraction of bare soil in many cells, thus decreasing available fuel for burning and, thus, fire danger<sup>28</sup>. Therefore, we see here a shift from a fire-dominated to a temperature-controlled ecosystem.

After its initial decline, the burnt area stabilized at a lower level and therefore indicated a saturation of the recovery process (Fig. S9). Forest biomass, however, needed more time to reach its potential maximum, but also, here, a clear saturation towards the end of the recovery phase is evident (Fig. 3b, S7). Therefore, vegetation, climate, and fire reached a new quasi-equilibrium in the Amazon forest, in which fire substantially delayed or prevented the regrowth of the Amazon basin.

Comparing recovery and control (no deforestation) experiments reveals that two very different and clearly separated stable

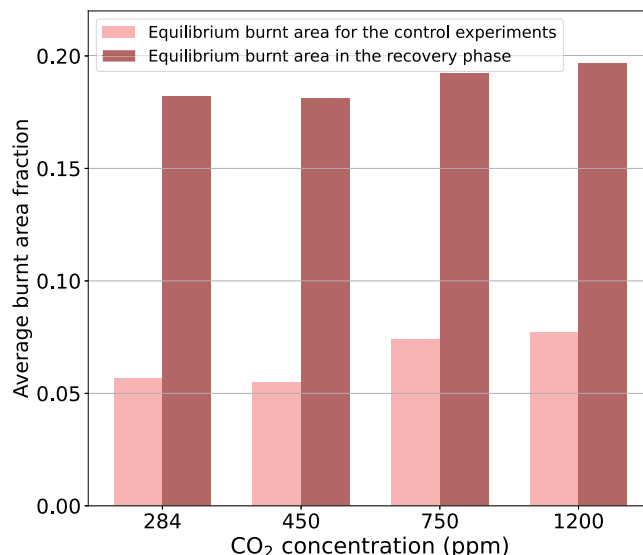


**Fig. 5 Bar plot of mean burnt area in the Amazon under different atmospheric CO<sub>2</sub> concentrations for the last 10 years of the recovery phase and their respective control experiments.** Burnt area is expressed as fractions of 0.5° lat × lon grid cells for which the average overall grid cell sizes in the Amazon basin was taken. Starting from grassland conditions, the mean burnt area was substantially higher than in the control experiments, for which a closed forest cover in the Amazon basin was simulated.

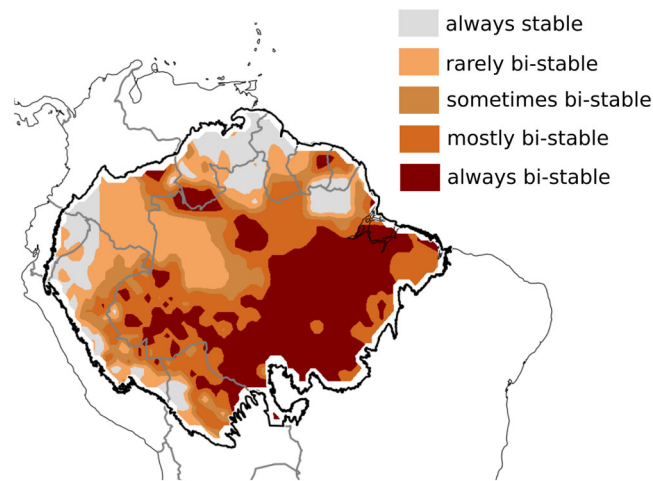


**Fig. 6 Bi-stability of forest cover and grassland in the Amazon forest.** Bi-stable regions can either be in the grassland or forest state under exactly the same climate and fire ignition conditions, depending on whether the scenario started from grassland (recovery phase) or from an intact Amazon forest (control experiment). The always stable area maintained a grassland or forest state for all experiments, while the rarely (sometimes, mostly, always) bi-stable areas showed bi-stability for one (two, three, four) of the experiments under different CO<sub>2</sub> concentrations.

states are possible for this important region of the Earth system in our model (Fig. 6): Despite having been forced with the same atmospheric CO<sub>2</sub> concentration and fire ignition data, the long-term trajectory of both simulations differed substantially. The attained state depended only on the extent of the Amazon forest cover at the beginning of the simulations. In contrast, the results of the control experiments (starting from an intact forest cover) showed that the ecosystem remained mostly intact even under strong climate impact and increased fire ignitions, which has been

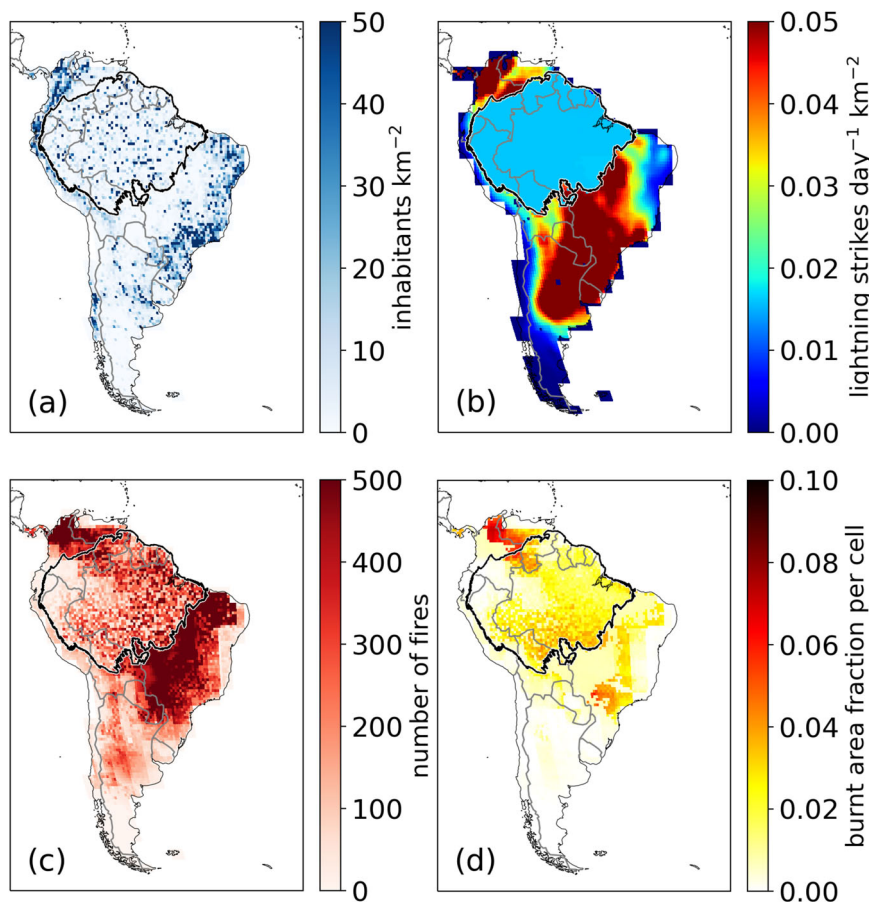


**Fig. 7** The effect of prescribed ignition sources in the Amazon biome on fire modeling in POEM. **a** Population density in inhabitants  $\text{km}^{-2}$ , **b** lightning strikes  $\text{day}^{-1} \text{km}^{-2}$ , **c** average monthly modeled number of fires per cell, **d** average monthly fraction of burnt area per cell.

shown previously<sup>33</sup>. The dependence of the long-term trajectory on the previous history (here: initial state) and thus irreversibility for certain conditions led to bi-stability between forest and grassland for a large area of the Amazon basin. While parts of the forest showed bi-stability for all tested  $\text{CO}_2$  concentrations (mostly in the eastern Amazon, always bi-stable in Fig. 6), the more complex large-scale pattern of no, partial or limited regrowth depended on the prevailing climate conditions (see Table 1). Therefore, the impact of deforestation on moisture recycling and vegetation dynamics varies in different regions of the Amazon basin. According to our study, there are bi-stable regions where a strong decline in moisture recycling (complete deforestation) could lead to vegetation not receiving enough water to grow quickly and suppress fires. This means that already deforested regions that fall within the bi-stable range in our simulations may have difficulty to regenerate on their own. In contrast, our model shows that it is more likely that the forest will regain its original state on its own in other areas (provided that moisture recycling does not decrease substantially).

**The role of human and natural ignitions.** The development of fire ignition sources plays an important role in predicting future fire regimes in the different biomes of South America. In the densely vegetated central Amazon forest, fire is currently a rare occurrence: The population density and the likelihood of humans igniting a fire are very low, and often zero. Fires are usually only observed along roads and at deforestation sites at the edge of the forest<sup>34</sup>. On the other hand, lightning ignitions are frequent in the Amazon, due to convective processes<sup>35</sup>, but usually, the forest is

too moist to start burning. Deforestation of the Amazon would, however, lead to non-linear changes in the number of potential ignitions in the Amazon region because human ignitions are closely connected to the expansion of treeless area<sup>34,36,37</sup>. Such a transition to grassland/land use would result in increased human ignitions similar to those observed today in the Cerrado, due to people migrating into the deforested areas. Large grassland regions would stimulate cattle ranching and areas, then easily accessible, would be converted into agricultural lands, connected by roads, thus increasing the number of potential ignition sources<sup>38</sup>. On the other hand, lightning activity might decrease, due to reduced convection over the deforested Amazon.

While realistic modeling of human ignitions in a deforested Amazon forest requires a socio-economic model (e.g., Copan: CORE<sup>39</sup>), here we assumed a population density in the Amazon basin constructed by choosing for each Amazon cell the population density of a randomly chosen cell in the Cerrado region (Fig. 7a and Methods). In doing so, we considered the possible increased population density of the Amazon after deforestation but also allow for variability, which is typical in already (partially) deforested regions. On the other hand, we decreased the number of lightning strikes by forcing the Amazon basin with average lightning data from the relatively low convection area of the Caatinga in northeast Brazil (Fig. 7b).

When comparing the fire-enabled with the respective control experiments, the forcing of increased population density and decreased lightning activity remained the same for all simulations (see Methods). While these ignitions are certainly unrealistic for the fully grown forest in the control experiments, it reinforces our result of the bi-stability in the Amazon basin: The fully grown

Amazon forest survives even at increased ignitions and elevated atmospheric CO<sub>2</sub>. Recovering from a deforestation event, however, fire-vegetation-climate interactions prevent the complete recovery into the forest state.

**Limitations of the modeling approach.** While most studies investigating tropical tipping and bi-stability rely on remote sensing data, conceptual models, or uncoupled models, we used here the fully biophysically coupled Earth system model POEM, with an embedded state-of-the-art, fire-enabled dynamic global vegetation model LPJmL. One of the main advantages of our model is that it can simulate the long-term dynamics of the Amazon forest under various scenarios of climate change and fire. Our model has a lower spatial resolution than most of the CMIP6 models, but it incorporates a sophisticated dynamic global vegetation model that accounts for the feedback between vegetation and climate (that are not accounted for in simpler modeling approaches<sup>15,20</sup>), as well as a process-based fire model that captures the effects of fire on the ecosystem<sup>25</sup>. These features are rare among the CMIP6 models and allow us to explore the possibility of an Amazon bi-stability and tipping, which has been a topic of interest for many years<sup>11,13</sup>, and to assess the potential for recovery of the forest under different levels of warming and fire disturbance.

Earth system models such as POEM are, however, tuned and calibrated to match historical data well, and projections into the future can suffer from large remaining process uncertainty<sup>22,40</sup>. Biases in the simulation of global climate could lead to an error propagation on the distribution of global vegetation, which in turn affects the carbon cycle, the water cycle, and the energy balance. In simulations of the coupled climate model inter-comparison phase 5 and 6 (CMIP<sup>40</sup>), carbon fluxes between biosphere and atmosphere, as well as surface temperature, differ by about 800 PgC globally and surface temperature by 2°C in an idealized emission scenario for 100 years<sup>41</sup>. These differences in global warming and vegetation carbon flux could strongly impact the results of a potential Amazon degradation or die-back. While POEM captures the general patterns of climate and vegetation and the performance is in the range of CMIP5 models (ref. <sup>25</sup>, S10–S12), the CO<sub>2</sub> fertilization effect in POEM could possibly be overestimated as it can be limited by other factors such as nutrient availability<sup>42</sup> or leaf cooling<sup>43</sup>, which are not accounted for in the current model version. Including both processes would lower the biomass increase under elevated CO<sub>2</sub> and could decrease biomass recovery. Furthermore, accounting for natural plant trait diversity, e.g., a continuum of tree rooting strategies, could reduce simulated drought stress and thus increase the potential forest re-establishment under a broader climatic range<sup>32</sup>.

In addition to uncertainties in the simulation of global climate and carbon cycle dynamics, also fire models are calibrated to match satellite observations of burned area and fire activity, with limited data in time and space<sup>44</sup>. Therefore, fire models may not capture the variability and trends of fire regimes in different regions and periods. This can lead to systematic errors and biases in the simulated fire regimes, especially before and after the satellite era. To improve the accuracy and reliability of fire models, a more process-based understanding of the drivers and impacts of fires is needed. Fire modeling in our study is also limited by the model resolution of POEM, which does not capture the heterogeneity of individual trees within a grid cell. Instead, it assumes an average tree individual that is representative of the entire cell. This affects the estimation of the burnt area, which is only available as a fraction of the cell area. Consequently, we cannot account for the variability of fire frequency among

different trees or forest plots. For example, if a cell has a burnt area of 10% per year, this implies a fire return interval of 10 years for the entire cell. However, this may not reflect the actual fire regime, as some parts of the cell may burn more frequently than others. We use LPJmL coupled with CM2Mc at a spatial resolution of 0.5 × 0.5 degrees, which is relatively fine for an Earth system model, but still coarse for capturing detailed fire dynamics. A higher spatial resolution would improve the representation of fire impacts on vegetation, but it would also increase the computational demand and limit the number of model experiments.

Due to substantial biases in simulated climate and vegetation patterns (Figs. S10–S12) as well as uncertainties associated with fire and Earth system modeling, it is not the aim of this study to simulate the exact velocity and pattern of vegetation recovery or to suggest concrete measures to safeguard the Amazon rainforest. We demonstrate in this study the potential impact of fire on the recovery of the Amazon rainforest, by applying well-chosen control experiments: (a) the recovery without fire and b) the trajectory of the Amazon rainforest with exactly the same fire/climate forcing but starting from an intact forest cover instead of grassland. As both control experiments yield a stable forest state, we can dismiss the conclusion that fire or climate change alone are strong enough to always lead to a grassland state in our model setup. Instead, the results suggest that the combined effect of fire and climate change in combination with the initial conditions is decisive. We conclude that fire is a key process determining potential forest recovery on regional scales. We demonstrated that climate-fire-vegetation feedback could lock vast parts of the Amazon in a treeless state. Comparisons of the control and deforested simulations revealed the potential bi-stability of regions within the Amazon and underscored the significance of initial conditions for the disturbance simulations.

Future studies could take into account a variety of deforestation scenarios, ranging from the present land cover pattern in the Amazon basin to the full deforestation scenario discussed in this paper, to further emphasize the danger of a potential fire-controlled lock-in effect in a state of no trees after deforestation. The size and location of the deforested region would most likely determine the likelihood of regeneration. The effects of various ignition scenarios on the potency of interactions between fire, vegetation, and climate could also be examined. Yet, a fully connected Earth system model would take a lot of computer power to apply to such a wide range of scenarios, which is outside the scope of this paper.

## Conclusions

Employing a fire-enabled Earth system model, this study demonstrated that fire could prevent the recovery of 56–82% of the Amazon forest (353–515 Mio ha, depending on atmospheric CO<sub>2</sub> concentration) after a large-scale deforestation event, showing a history-dependent bi-stability of the Amazon basin ecosystem. Several positive feedback loops, for instance, the reduction of evapotranspiration and precipitation related to tree loss, increased temperatures, and fire activity, stabilized the grassland state in more than half of the Amazon basin in our model simulations. On the other hand, with deactivated fire disturbance, the forest was able to almost completely recover from the grassland state.

Therefore, our model simulations show that fire is a crucial factor in evaluating the potential future forest recovery. Fire disturbance, along with large-scale deforestation, can create a lock-in effect that prevents the forest from returning to its original state. This implies that the system state could change dramatically if deforestation and climate change surpass certain

thresholds. Our results provide another strong argument for the need to protect the Amazon forests, by stopping deforestation and reducing global CO<sub>2</sub> emissions as they question the feasibility of future reforestation measures without fire control.

## Methods

**Model description and input data.** We used the coupled Earth system model Potsdam Earth Model (POEM, in the configuration CM2Mc-LPJmL v1.0<sup>25</sup>), combining the relatively coarse but fast atmosphere and ocean model CM2Mc<sup>45</sup> with the state-of-the-art dynamic global vegetation model (DGVM) LPJmL5.0-FMS<sup>26,46</sup>, employing the process-based fire model SPITFIRE<sup>27</sup>. CM2Mc is a coarser configuration of the Climate Model 2 (CM2)<sup>47</sup> model framework developed by the Geophysical Fluid Dynamics Laboratory (GFDL), coupled to the Modular Ocean Model 5 (MOM5) at a coarse spatial resolution of 3° × 3.75° latitude-longitude<sup>45</sup>. The original model configuration includes the global atmosphere and land model AM2-LM2 or AM2-LM<sup>48</sup> with static vegetation. In the newly developed CM2Mc-LPJmL configuration, the static land model LM is replaced by the dynamic global vegetation model LPJmL, while keeping MOM5 and AM2 dynamically coupled. All model components are connected via GFDL's flexible modeling system (FMS), which is a software framework to support the efficient software development, coupling, application, and flux exchange of its land, atmosphere, and ocean components<sup>49</sup>.

The Lund–Potsdam–Jena managed Land version model LPJmL5<sup>26,46</sup> is an extensively validated and established process-based DGVM, which globally simulates the water fluxes, surface energy balance, carbon fluxes, and stocks for both, natural and managed vegetation forced by climate, soil, and land use input data. To simulate vegetation composition, LPJmL explicitly considers the establishment, growth, competition, and mortality of plant functional types (PFT) in natural vegetation, which changes the foliar projective cover (FPC) of competing PFTs. The establishment and survival of different PFTs is controlled through bioclimatic limits and the effects of productivity, heat, and fire on plant mortality. These processes enable LPJmL to investigate several feedback mechanisms in the biosphere, for example, between vegetation cover and fire. For the study region of northern South America, three PFTs are possible in the tropical climate, which are the tropical evergreen tree, the tropical raingreen tree, and tropical grass. While the raingreen tree is slightly more fire resistant, the evergreen has advantages in a wet climate, as in the Amazon rainforest. Under very dry and hot conditions, no tree PFTs can establish and the grass PFT is growing, while under extreme dry and hot conditions, no PFT can establish, resulting in bare soil. LPJmL simulates water balance<sup>50</sup>, agriculture<sup>51</sup>, wildfires in natural vegetation (SPITFIRE)<sup>27</sup>, permafrost<sup>52</sup>, and specified multiple climate drivers on phenology<sup>53,54</sup>. Recently, by using an optimization approach and by developing a new fire danger index, a more realistic fire representation has been obtained<sup>28</sup>. We applied the optimized and improved SPITFIRE in this study.

The coupling between atmosphere and biosphere in POEM consists of the variables canopy humidity, soil and canopy temperature, roughness length, and albedo, which are calculated within LPJmL but interact with the atmosphere in a temporal resolution of one hour<sup>25</sup>. These variables are passed to the coupling software FMS, which provides LPJmL with the necessary climatic input, i.e., air temperature, radiation, and precipitation. While the spatial resolution of the atmosphere and ocean is 3° × 3.75° latitude-longitude, LPJmL uses its native resolution of a 0.5° × 0.5° latitude-longitude grid. The variables exchanged in both directions are interpolated by FMS, which guarantees the conservation of all scalar and vector fields. Thus, the atmospheric input in one grid cell is distributed over several biosphere grid cells.

For the coupling of LPJmL into CM2Mc, several important processes had to be adjusted within LPJmL, which included the use of the Penman-Monteith scheme<sup>55</sup> for the calculation of potential evapotranspiration and the modeling of canopy humidity. Furthermore, the calculation of surface temperature by employing a simple energy balance parameterization was included. Roughness lengths and albedo were calculated as in stand-alone LPJmL<sup>26</sup>. A large negative temperature bias in the northern latitudes was counteracted by the addition of a more detailed parameterization of the sublimation<sup>56</sup>. A small wrapper library has been developed for the data exchange between LPJmL and the FMS domain, to make the LPJmL grid compatible with FMS.

A more detailed description of the biophysical coupling of LPJmL into CM2Mc and the published code can be found in a separate publication in Geoscientific Model Development<sup>25</sup>. A short evaluation of the standard model, equivalent to ref. <sup>25</sup> can be found in Figs. S10–S12.

**Experimental setup.** To investigate the impact of fire and climate change on the potential regrowth of the Amazon forest after a large-scale deforestation event, we applied POEM in a series of model experiments:

All experiments share the same spinup, which is consistent with ref. <sup>25</sup>: After a 5000-year stand-alone LPJmL spin-up, a second fully coupled spin-up under pre-industrial conditions without land use was performed for 1500 model years (Fig. 1 and S13). In this way, we ensured that the model starts from a consistent equilibrium between the long-term soil carbon pool, vegetation, ocean, and climate. After this spin-up period, the whole biome of the Amazon forest was replaced by

natural grassland, i.e., all trees were cut and no tree establishment was allowed, while the atmospheric CO<sub>2</sub> concentration was kept at different constant values. To get the model close to a new equilibrium after this strong disturbance, pure grassland was simulated for 250 years (grassland phase). In the following simulation phase of another 250 years, trees were allowed to regrow (recovery phase). Both, the grassland- and recovery phases, were conducted for four different atmospheric CO<sub>2</sub> levels, which remained constant over time: 284 (pre-industrial), 450, 750, and 1200 ppm, and each with and without enabled fire disturbance. Furthermore, we conducted the respective control experiments, where potential natural vegetation without the deforestation of the Amazon forest was simulated, also with and without fire, each set under different CO<sub>2</sub> concentrations. The control experiments started from the same spinup and were simulated for 250 years, to reach an equilibrium between fire, vegetation, and climate.

**Forcing of ignition sources.** To account for the fact, that population density in the deforested Amazon would increase, we assigned each cell in the Amazon basin the population density and the inclination of humans to set a fire<sup>27</sup> of a randomly chosen cell in the Cerrado region (Fig. 7). On the other hand, we substituted the number of lightning strikes by forcing the Amazon basin with average lightning data from the relatively low convection area of the Caatinga in northeast Brazil. In the different experiments in this study, all setups with activated fire disturbance have the same forcing of human and natural ignition sources. By this, we make sure that the results of the scenario run and the control runs are comparable.

## Data availability

The data used for the analysis and creation of the figures in this paper is publicly available under the Creative Commons Attribution 4.0 International license at Zenodo (<https://doi.org/10.5281/zenodo.8028061>)<sup>57</sup>.

## Code availability

The model code for POEM used in this study, and the corresponding Python3 scripts for the creation of the figures is publicly available under the Creative Commons Attribution 4.0 International license at Zenodo (<https://doi.org/10.5281/zenodo.8028061>)<sup>58</sup>.

Received: 6 October 2022; Accepted: 23 June 2023;

Published online: 11 July 2023

## References

1. Brovkin, V., Raddatz, T., Reick, C. H., Claussen, M. & Gayler, V. Global biogeophysical interactions between forest and climate. *Geophys. Res. Lett.* **36**, L07405 (2009).
2. Marengo, J. A. et al. Changes in climate and land use over the Amazon region: current and future variability and trends. *Front. Earth Sci.* **6** (2018).
3. Brandon, K. Ecosystem services from tropical forests: review of current science. *Center for Global Development Working Paper No. 380*. Available at SSRN: <https://ssrn.com/abstract=2622749> (2014).
4. Cochrane, M. A. & Laurance, W. F. Synergisms among fire, land use, and climate change in the Amazon. *Ambio* **37**, 522–527 (2008).
5. Beuchle, R. et al. Land cover changes in the Brazilian Cerrado and Caatinga biomes from 1990 to 2010 based on a systematic remote sensing sampling approach. *Appl. Geogr.* **58**, 116–127 (2015).
6. Malhi, Y. et al. Climate change, deforestation, and the fate of the Amazon. *Science* **319**, 169–172 (2008).
7. Davidson, E. A. et al. The Amazon basin in transition. *Nature* **481**, 321–328 (2012).
8. Nobre, C. A. et al. Land-use and climate change risks in the Amazon and the need of a novel sustainable development paradigm. *Proc. Natl Acad. Sci. USA* **113**, 10759–10768 (2016).
9. Brando, P. M. et al. The gathering firestorm in southern Amazonia. *Sci. Adv.* **6**, eaay1632 (2020).
10. Gatti, L. V. et al. Amazonia as a carbon source linked to deforestation and climate change. *Nature* **595**, 388–393 (2021).
11. Cox, P. M. et al. Amazonian forest dieback under climate-carbon cycle projections for the 21st century. *Theor. Appl. Climatol.* **78**, 137–156 (2004).
12. Boulton, C. A., Good, P. & Lenton, T. M. Early warning signals of simulated Amazon rainforest dieback. *Theor. Ecol.* **6**, 373–384 (2013).
13. Parry, I., Ritchie, P. & Cox, P. Evidence of Amazon rainforest dieback in CMIP6 models. Preprint at arXiv:2203.11744 (2022).
14. Lovejoy, T. E. & Nobre, C. Amazon tipping point. *Sci. Adv.* **4** (2018).
15. Lasslop, G., Brovkin, V., Reick, C. H., Bathiany, S. & Kloster, S. Multiple stable states of tree cover in a global land surface model due to a fire-vegetation feedback. *Geophys. Res. Lett.* **43**, 6324–6331 (2016).



16. Zemp, D. C., Schleussner, C. F., Barbosa, H. M. J. & Rammig, A. Deforestation effects on Amazon forest resilience. *Geophys. Res. Lett.* **44**, 6182–6190 (2017).
17. Boers, N., Marwan, N., Barbosa, H. M. J. & Kurths, J. A deforestation-induced tipping point for the South American monsoon system. *Sci. Rep.* **7**, 1–9 (2017).
18. Rammig, A. et al. Estimating the risk of Amazonian forest dieback. *New Phytol.* **187**, 694–706 (2010).
19. Hirota, M., Holmgren, M., Van Nes, E. H. & Scheffer, M. Global resilience of tropical forest and savanna to critical transitions. *Science* **334**, 232–235 (2011).
20. Baudena, M., D'Andrea, F. & Provenzale, A. An idealized model for tree-grass coexistence in savannas: the role of life stage structure and fire disturbances. *J. Ecol.* **98**, 74–80 (2010).
21. Staal, A. et al. Forest-rainfall cascades buffer against drought across the Amazon. *Nat. Clim. Change* **8**, 539–543 (2018).
22. Kattsov, V. et al. Evaluation of climate models (AR5). In *Climate Change 2013 The Physical Science Basis: Working Group I Contribution to the Fifth Assessment Report of the Intergovernmental Panel on Climate Change* 741–866 (Cambridge Univ. Press, 2013).
23. Staal, A. et al. Hysteresis of tropical forests in the 21st century. *Nat. Commun.* **11**, 4978 (2020).
24. Zemp, D. C. et al. Self-amplified Amazon forest loss due to vegetation-atmosphere feedbacks. *Nat. Commun.* **8**, 1–10 (2017).
25. Drüke, M. et al. CM2Mc-LPJmL v1.0: biophysical coupling of a process-based dynamic vegetation model with managed land to a general circulation model. *Geosci. Model Dev.* **14**, 4117–4141 (2021).
26. Schaphoff, S. et al. LPJmL4 - a dynamic global vegetation model with managed land - Part 1: model description. *Geosci. Model Dev.* **11**, 1343–1375 (2018).
27. Thonicke, K. et al. The influence of vegetation, fire spread and fire behaviour on biomass burning and trace gas emissions: results from a process-based model. *Biogeosciences* **7**, 1991–2011 (2010).
28. Drüke, M. et al. Improving the LPJmL4-SPITFIRE vegetation-fire model for South America using satellite data. *Geosci. Model Dev.* **12**, 5029–5054 (2019).
29. Sampaio, G. et al. Regional climate change over eastern Amazonia caused by pasture and soybean cropland expansion. *Geophys. Res. Lett.* **34**, 1–7 (2007).
30. Gkatsopoulos, P. A methodology for calculating cooling from vegetation evapotranspiration for use in urban space microclimate simulations. *Procedia Environ. Sci.* **38**, 477–484 (2017).
31. Unger, N. Human land-use-driven reduction of forest volatiles cools global climate. *Nat. Clim. Change* **4**, 907–910 (2014).
32. Sakschewski, B. et al. Variable tree rooting strategies are key for modelling the distribution, productivity and evapotranspiration of tropical evergreen forests. *Biogeosciences* **18**, 4091–4116 (2021).
33. Drüke, M. et al. Climate-induced hysteresis of the tropical forest in a fire-enabled Earth system model. *Eur. Phys. J. Spec. Top.* **230**, 3153–3162 (2021).
34. Cano-Crespo, A., Traxl, D. & Thonicke, K. Spatio-temporal patterns of extreme fires in Amazonian forests. *Eur. Phys. J. Spec. Top.* **230**, 3033–3044 (2021).
35. Pinto, I. R. & Pinto, J. Cloud-to-ground lightning distribution in Brazil. *J. Atmos. Solar-Terrestrial Phys.* **65**, 733–737 (2003).
36. Barlow, J. & Peres, C. A. Fire-mediated dieback and compositional cascade in an Amazonian forest. *Philos. Trans. R. Soc. B Biol. Sci.* **363**, 1787–1794 (2008).
37. Cochran, M. A. Fire science for rainforests. *Nature* **421**, 913–919 (2003).
38. Butsic, V., Kelly, M. & Moritz, M. A. Land use and wildfire: a review of local interactions and teleconnections. *Land* **4**, 140–156 (2015).
39. Donges, J. F. et al. Earth system modeling with endogenous and dynamic human societies: the copan: CORE open World-Earth modeling framework. *Earth Syst. Dyn.* **11**, 395–413 (2020).
40. Friedlingstein, P. et al. Uncertainties in CMIP5 climate projections due to carbon cycle feedbacks. *J. Clim.* **27**, 511–526 (2014).
41. Arora, V. K. et al. Carbon-concentration and carbon-climate feedbacks in CMIP6 models and their comparison to CMIP5 models. *Biogeosciences* **17**, 4173–4222 (2020).
42. Davies-Barnard, T. et al. Nitrogen cycling in CMIP6 land surface models: progress and limitations. *Biogeosciences* **17**, 5129–5148 (2020).
43. Medlyn, B. E. et al. Temperature response of parameters of a biochemically based model of photosynthesis. II. A review of experimental data. *Plant Cell Environ.* **25**, 1167–1179 (2002).
44. Hantson, S. et al. The status and challenge of global fire modelling. *Biogeosciences* **13**, 3359–3375 (2016).
45. Galbraith, E. D. et al. Climate variability and radiocarbon in the CM2Mc earth system model. *J. Clim.* **24**, 4230–4254 (2011).
46. Von Bloh, W. et al. Implementing the nitrogen cycle into the dynamic global vegetation, hydrology, and crop growth model LPJmL (version 5.0). *Geosci. Model Dev.* **11**, 2789–2812 (2018).
47. Milly, P. C. & Shmakin, A. B. Global modeling of land water and energy balances. Part I: the land dynamics (LaD) model. *J. Hydrometeorol.* **3**, 283–299 (2002).
48. Anderson, J. L. et al. The new GFDL global atmosphere and land model AM2-LM2: evaluation with prescribed SST simulations. *J. Clim.* **17**, 4641–4673 (2004).
49. Balaji, V. The FMS manual: a developer's guide to the GFDL Flexible Modeling System. <http://www.gfdl.noaa.gov/~vb/FMSManual/FMSManual.html> (2022).
50. Gerten, D., Schaphoff, S., Haberlandt, U., Lucht, W. & Sitch, S. Terrestrial vegetation and water balance - hydrological evaluation of a dynamic global vegetation model. *J. Hydrol.* **286**, 249–270 (2004).
51. Bondeau, A. et al. Modelling the role of agriculture for the 20th century global terrestrial carbon balance. *Glob. Change Biol.* **13**, 679–706 (2007).
52. Schaphoff, S. et al. Contribution of permafrost soils to the global carbon budget. *Environ. Res. Lett.* **8**, 14026 (2013).
53. Forkel, M. et al. Identifying environmental controls on vegetation greenness phenology through model-data integration. *Biogeosciences* **11**, 7025–7050 (2014).
54. Forkel, M. et al. Constraining modelled global vegetation dynamics and carbon turnover using multiple satellite observations. *Sci. Rep.* **9**, 18757 (2019).
55. Monteith, J. L. Rothamsted Repository Download. *Symposia of the Society for Experimental Biology* 205–234 (1965).
56. Gelfan, A. N., Pomeroy, J. W. & Kuchment, L. S. Modeling forest cover influences on snow accumulation, sublimation, and melt. *J. Hydrometeorol.* **5**, 785–803 (2004).
57. Drüke, M. Data for Drüke et al. 2023, Communication Earth and Environment. <https://zenodo.org/record/8027823> (2023).
58. Drüke, M. Model code and scripts for Drüke et al. 2023, Communication Earth and Environment. <https://zenodo.org/record/8028061> (2023).

## Acknowledgements

This work has been carried out within the framework of the project POEM-PBSim: A Simulator for Earth's Planetary Boundaries, funded by the VolkswagenStiftung at the Potsdam Institute for Climate Impact Research. M.D. gratefully acknowledges the financial support of the VolkswagenStiftung and the International Research Training Group (IRTG) 1740/TRP 2015/50122-0 project funded by Deutsche Forschungsgemeinschaft (DFG) and São Paulo Research Foundation (FAPESP). M.B. acknowledges funding from the European Union's Horizon 2020 FirEURisk (Grant Agreement no. 101003890). B.S. gratefully acknowledges funding from Waldklimafonds by the Federal Ministry of Food and Agriculture and the Federal Ministry for the Environment, Nature Conservation, Building and Nuclear Safety, Germany (Project WaldSpektrum, support code 2219WK39A4). B.S. gratefully acknowledges funding from the Earth Commission. The Earth Commission is hosted by Future Earth and is the science component of the Global Commons Alliance. The Global Commons Alliance is a sponsored project of Rockefeller Philanthropy Advisors, with support from Oak Foundation, MAVA, Porticus, Gordon and Betty Moore Foundation, Herlin Foundation, and the Global Environment Facility. The Earth Commission is also supported by the Global Challenges Foundation. The authors gratefully acknowledge the European Regional Development Fund (ERDF), the German Federal Ministry of Education and Research, and the Land Brandenburg for supporting this project by providing resources on the high-performance computer system at the Potsdam Institute for Climate Impact Research. The authors are grateful to the whole POEM development team at the Potsdam Institute for Climate Impact Research.

## Author contributions

M.D. conceived the study. M.D. performed and analyzed the simulations with support from B.S. and W.v.B. M.D., B.S., W.v.B., M.B., W.L., and K.T. contributed to discussions and interpretation of the results. M.D., B.S., and M.B. created the figures and the supplementary video. M.D. wrote most of the paper with input from B.S. and further contributions by all co-authors.

## Funding

Open Access funding enabled and organized by Projekt DEAL.

## Competing interests

The authors declare no competing interests.

## Additional information

**Supplementary information** The online version contains supplementary material available at <https://doi.org/10.1038/s43247-023-00911-5>.

**Correspondence** and requests for materials should be addressed to Markus Drüke.

**Peer review information** *Communications Earth & Environment* thanks the anonymous reviewers for their contribution to the peer review of this work. Primary Handling Editors: Yongqiang Liu and Aliénor Lavergne. A peer review file is available

**Reprints and permission information** is available at <http://www.nature.com/reprints>

**Publisher's note** Springer Nature remains neutral with regard to jurisdictional claims in published maps and institutional affiliations.



**Open Access** This article is licensed under a Creative Commons Attribution 4.0 International License, which permits use, sharing, adaptation, distribution and reproduction in any medium or format, as long as you give appropriate credit to the original author(s) and the source, provide a link to the Creative Commons licence, and indicate if changes were made. The images or other third party material in this article are included in the article's Creative Commons licence, unless indicated otherwise in a credit line to the material. If material is not included in the article's Creative Commons licence and your intended use is not permitted by statutory regulation or exceeds the permitted use, you will need to obtain permission directly from the copyright holder. To view a copy of this licence, visit <http://creativecommons.org/licenses/by/4.0/>.

© The Author(s) 2023